Finite Element Analysis of Adaptive Trusses with Shape Memory Alloy Members

Yutaka Toi and Kazunori Tsukamoto

Abstract—**A finite element procedure for three-dimensional adaptive trusses using shape memory alloys is formulated in the present study, in which the extended form of Brinson's constitutive equation considering asymmetric tensile and compressive behavior is expressed in a tangentially incremental form. The validity of the present computational modeling is demonstrated by conducting numerical studies for the superelastic, shape memory behaviors of two-bar, nine-bar and twenty eight-bar adaptive trusses subjected to load and temperature changes. The proposed computational procedure is expected to be useful for the optimum design of the adaptive trusses with shape memory alloy bars.**

Index Terms—**Finite Element Method, Adaptive Structure, Framed Structure, Shape Memory Materials, Smart Materials**

I. INTRODUCTION

Adaptive truss structures, which can control their mechanical properties such as stiffness and deformation, are applicable to parabola antennas and space structures. Wire actuators and shape memory alloys (SMAs) have been studied as control mechanisms [1], [2]. Development of a practical computational tool is necessary for the efficient design of adaptive trusses.

A finite element analysis procedure for the adaptive trusses using SMA members is formulated in the present study. Its validity is illustrated by some numerical examples. Bandeira et al. [2] conducted finite element analysis of the adaptive trusses using SMA members, employing the constitutive equation by Paiva et al. [3]. Their analysis is based on the incremental constitutive equation in an initial stress form, only for two-dimensional trusses and neglects the asymmetry of tensile and compressive behaviors.

The phenomenological and simple constitutive equation given by Brinson [4] is extended to consider the asymmetric tensile and compressive behaviors [5] in the present finite element analysis procedure. The numerically stable, incremental constitutive equation in a tangential stiffness form [6] is derived and applied to the incremental finite element analysis of general three-dimensional adaptive trusses.

A finite element analysis procedure for SMA trusses is formulated in Section 2. Results of the finite element

analysis of adaptive trusses are described in Section 3. Section 4 contains concluding remarks.

II. FINITE ELEMENT ANALYSIS PROCEDURE OF SHAPE MEMORY ALLOY TRUSSES

A. Constitutive Equation

The mechanical property of SMA is schematically shown in Fig. 1. Fig. 1(a) and Fig. 1(b) are the stress-strain curve and the relation between critical transformation stresses and temperature respectively, in which the superelastic behavior (bold line arrow) and the shape memory effect behavior (broken line arrow) are shown.

In Fig. 1, the following notations are used: σ; the stress, ε; the strain, T; temperature, σ_f^{cr} and σ_s^{cr}; the finishing and starting critical stress for martensite transformation, M_f and M_s; the finishing and starting temperature for martensite transformation, A_s and A_f; the starting and finishing temperature for austenite transformation. In Fig. 1(b), σ_f^{cr} and σ_f^{cr} are assumed to be constant in the case of $T < M_s$ according to Brinson's formulation [4]. C_{M_s} and C_{M_f} are the gradients in the relations between the finishing and starting critical stress for martensite transformation and the temperature. C_{A_s} and C_{A_f} are the gradients in the relations between the starting and finishing critical stress for austenite transformation and the temperature. $C_{M_s} = C_{M_f} = C_M$ and $C_{A_s} = C_{A_f} = C_A$ are assumed in the present analysis.

When the stress is loaded and unloaded at the temperature lower than A_f ($M_f < M_s < T < A_s < A_f$ here) in Fig. 1(b), the inverse (austenite) transformation for the strain generated by the martensite transformation does not finish and leaves the residual strain (ε_{res}) as shown in Fig. 1(a). Heating to the temperature higher than A_f, the austenite transformation finishes and the strain disappears as shown in Fig. 1(a). Even when heating sufficiently without unloading of the stress, the strain generated by the martensite transformation disappears although the elastic strain remains. This is the outline of the shape memory effect. In the case of $T > A_f$, the superelastic behavior as shown in Fig. 1(a) takes place as the inverse transformation finishes.

The one-dimensional stress-strain relation of SMA is generally expressed by the following equation [4]:

$$\sigma - \sigma_0 = E(\xi)\varepsilon - E(\xi_0)\varepsilon_0 + \Omega(\xi)\xi_S - \Omega(\xi_0)\xi_{S0}$$
$$+ \theta(T - T_0)$$

(1)

where E ; Young's modulus, Ω ; the transformation coefficient, ξ_S ; the stress-induced martensite volume fraction, θ ; the elastic thermal coefficient, T ; temperature. The subscript "0" indicates initial values.

Ω is expressed as follows:

$$\Omega = -\varepsilon_L E$$

(2)

where ε_L is the maximum residual strain.

Young's modulus E is a function of the martensite volume fraction ξ , which is given by the following equation:

$$E = E_a + \xi(E_m - E_a)$$

(3)

where E_m and E_a are Young's modulus of martensite phase and austenite phase, respectively.

The martensite volume fraction ξ is expressed by the following equation:

$$\xi = \xi_S + \xi_T$$

(4)

where ξ_T is the temperature-induced martensite volume fractioin. ξ, ξ_S and ξ_T are functions of the temperature T and the stress σ .

In order to consider the asymmetric tensile and compressive behavior, the evolution equations for ξ, ξ_S and ξ_T are expressed by Drucker-Prager's equivalent stress in which the hydrostatic pressure term is added to von Mises' equivalent stress.

$$\sigma_{eq}^{DP} = \sigma_{eq}^{M} + 3\beta\sigma_H$$

(5)

where β is a material parameter. σ_H is the hydrostatic pressure given by the following equation:

$$\sigma_H = \frac{1}{3}\left(\sigma_x + \sigma_y + \sigma_z\right)$$

(6)

In one-dimensional case, the equivalent stress in eq. (5) is expressed as follows:

$$\sigma_{eq}^{DP} = \beta\sigma + |\sigma|$$

(7)

Substituting eq. (7) into the evolution equation for ξ, ξ_S and ξ_T given by Brinson [4], the evolution equation for the martensite and austenite transformation can be obtained.

The stress-strain relation given in eq. (1) can be expressed in a differential form as follows:
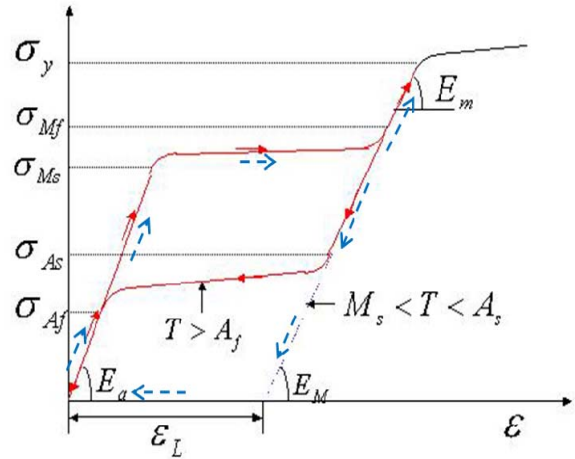
$$d\sigma = dE\varepsilon + Ed\varepsilon + d\Omega\xi_s + \Omega d\xi_s + \theta dT$$
$$= \frac{dE}{d\xi}\left(\frac{\partial\xi}{\partial\sigma}d\sigma + \frac{\partial\xi}{\partial T}dT\right)\varepsilon + Ed\varepsilon + \frac{d\Omega}{dE}\frac{dE}{d\xi}\left(\frac{\partial\xi}{\partial\sigma}d\sigma + \frac{\partial\xi}{\partial T}dT\right)\xi_s$$
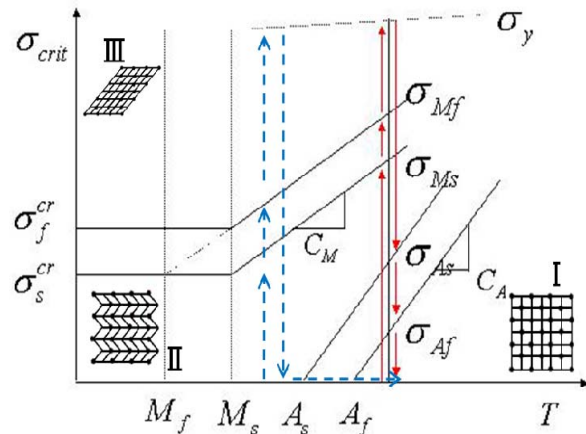$$+ \Omega\left(\frac{\partial\xi_s}{\partial\sigma}d\sigma + \frac{\partial\xi_s}{\partial T}dT\right) + \theta dT$$

(8)

The incremental form of stress-strain relation can be derived as follows:

$$\left[1 - \frac{dE}{d\xi}\frac{\partial\xi}{\partial\sigma}\varepsilon - \frac{d\Omega}{dE}\frac{dE}{d\xi}\frac{\partial\xi}{\partial\sigma}\xi_s - \Omega\frac{\partial\xi_s}{\partial\sigma}\right]d\sigma$$
$$= Ed\varepsilon + \left[\frac{dE}{d\xi}\frac{\partial\xi}{\partial T}\varepsilon + \frac{d\Omega}{dE}\frac{dE}{d\xi}\frac{\partial\xi}{\partial T}\xi_s + \Omega\frac{\partial\xi_s}{\partial T} + \theta\right]dT$$

(9)

(a) Superelastic behavior and shape memory effect

(b) Critical stresses for transformation vs. temperature

Fig.1 Mechanical properties of shape memory alloys

Therefore the stress-strain relation for the finite element analysis can be written as follows:

$$\{\Delta\sigma\} = [D_{se}]\left(\{\Delta\varepsilon\} - \{\Delta\varepsilon_{se}\}\right)$$

(10)

Details of eq. (10) are given in [5].

B. *Finite Element Analysis Procedure*

Based on the total Lagrangian approach [6], the finite element analysis procedure for a truss element is formulated assuming finite deformation.

Referring to Fig. 2, the displacement field in the three-dimensional truss element is assumed by the following equations:

$$u(z) = \left(1 - \frac{z}{l}\right)u_i + \frac{z}{l}u_j$$

(11a)

$$v(z) = \left(1 - \frac{z}{l}\right)v_i + \frac{z}{l}v_j$$

(11b)

$$w(z) = \left(1 - \frac{z}{l}\right)w_i + \frac{z}{l}w_j$$

(11c)

where $u(z)$ and $v(z)$ are the lateral displacements. $w(z)$ is the axial displacement.

The incremental strain-displacement relation is assumed as follows:

$$\Delta \varepsilon_z = \frac{d\Delta w}{dz} + \frac{du}{dz}\frac{d\Delta u}{dz} + \frac{dv}{dz}\frac{d\Delta v}{dz}$$
$$+ \frac{1}{2}\left[\left(\frac{d\Delta u}{dz}\right)^2 + \left(\frac{d\Delta v}{dz}\right)^2\right]$$

(12)

Equation (12) considers the nonlinear terms with respect to the lateral displacements, neglecting the nonlinear term with respect to the axial displacement.

The relation between the linear component of the strain increment and the nodal displacement increments is expressed in a matrix form as follows:

$$\{\Delta \varepsilon\} = [\overline{B}]\{\Delta d\} = ([B_0] + [B_L])\{\Delta d\}$$ (13)

where the following notations are used: $[\overline{B}]$; the strain-nodal displacement matrix, $[B_0]$; the strain-nodal displacement matrix without the influence of the initial displacements, $[B_L]$; the strain-nodal displacement matrix with the influence of the initial displacements, $\{\Delta d\}$; the nodal displacement increment vector ($\lfloor d \rfloor = \lfloor u_i\, v_i\, w_i\, u_j\, v_j\, w_j \rfloor$).

The finite element formulation based on the virtual work principle using the constitutive equation outlined in Subsection II.A leads to the incremental element stiffness equation as follows:

$$([k_0] + [k_L] + [k_G])\{\Delta u\} = \{\Delta f\} + \{\Delta f_{se}\} + \{f_R\}$$ (14)

where

$$[k_0] = \int_{V^e} [B_0]^T [D_{se}][B_0] dV^{(0)}$$

(15)

$$[k_L] = \int_{V^e} \left([B_0]^T[D_{se}][B_L] + [B_L]^T[D_{se}][B_0] + [B_L]^T[D_{se}][B_L]\right) dV^{(0)}$$

(16)

$$[k_G] = \int_{V^e} [G]^T [S][G] dV^{(0)}$$

(17)

$$\{\Delta f_{se}\} = \int_{V^e} [\overline{B}]^T [D_{se}]\{\Delta \varepsilon_{se}\} dV^{(0)}$$

(18)

The following notations are used in the equations: $[k_0]$; the incremental stiffness matrix, $[k_L]$; the initial displacement matrix, $[k_G]$; the initial stress matrix, $\{\Delta f\}$; the external force increment vector, $\{\Delta f_{se}\}$; the apparent external force increment vector due to the superelasticity and shape memory effect, $\{f_R\}$; the unbalanced force vector, $[D_{se}]$; the superelastic stress-strain matrix, $\{\Delta \varepsilon_{se}\}$; the initial strain

vector due to the superelasticity and shape memory effect, $[G]$; the gradient matrix, $[S]$; the stress matrix, V^e; the element volume.

The present formulation is applicable to simulations of the superelastic and shape memory effect responses of the general three-dimensional adaptive trusses using SMA members subjected to arbitrary load and temperature histories.
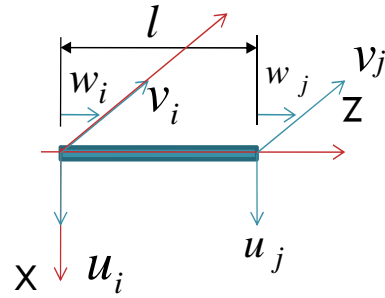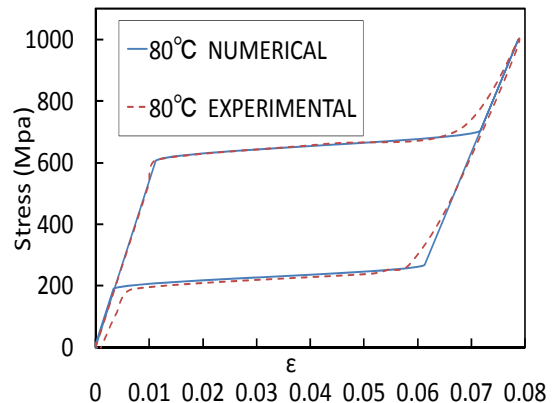

Fig.2 Truss element

Table 1.Material constants for SMA

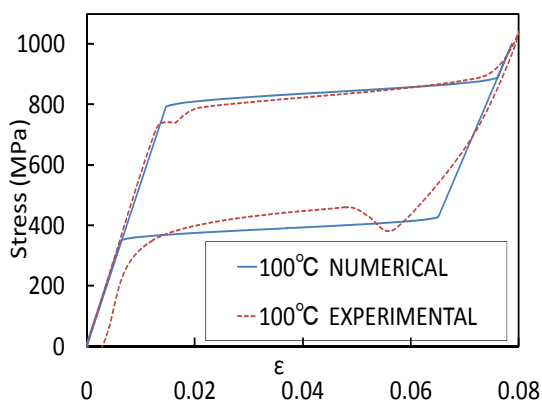|	
Modulus	E_a=54GPa
	E_m=42GPa
	E_S=200GPa
Transformation temperatures	M_f=10℃
	M_s= 20℃
	A_s= 46.25℃
	A_f=56.25℃
Transformation constants	C_M=9.25MPa/℃
	C_A=8.0MPa/℃
	σ_s^{cr}=50MPa
	C. σ_f^{cr}=150MPa
Maximum residual strain	ε_L=0.055

Fig.3 Stress-strain curves at 80℃(upper) and 100℃(lower)

III. FINITE ELEMENT ANALYSIS OF ADAPTIVE TRUSSES

A. Identification of Material Constants

The material constants of SMA defined in Subsection 2.1 have been determined as shown in Table 1, based on the experimental results by Tobushi et al. [7]. In Table 1, E_s is Young's modulus of steel which is assumed to be linearly elastic. It is assumed that $\beta = 0.15$ or $\beta = 0$ in eq. (7). Figure 3 shows the identified stress-strain curves at 80℃ and 100℃ compared with the experimental results by Tobushi et al. [7].

B. Two-Dimensional Two-Bar Truss

The two-dimensional two-bar adaptive truss as shown in Fig. 4 has been analyzed by using the material constants identified in Subsection Ⅲ.A. The members ① and ② are both SMA with a cross section of 1cm². The load F(t) increases at t=0~1.0 and keeps constant at t=1.0~2.0. The temperature keeps a constant value smaller than M_f at t=0~1.0, rises over A_f at t=1.0~2.0 and returns back at t=2.0~3.0. The present analysis considers the asymmetric tensile and compressive behavior, assuming $\beta = 0.15$ in eq. (7).

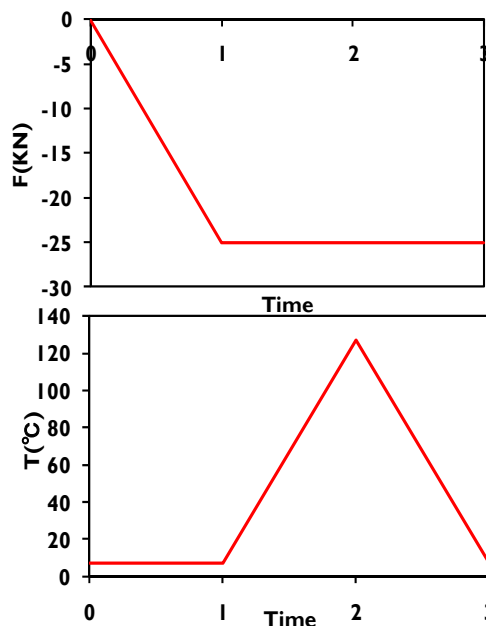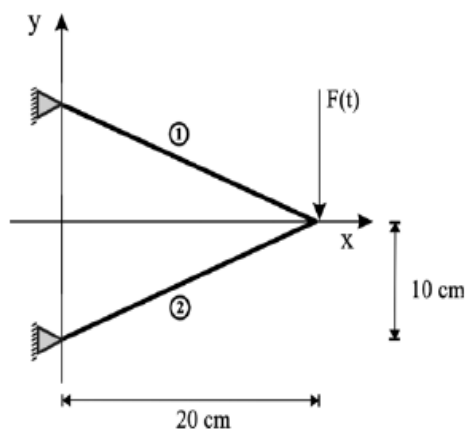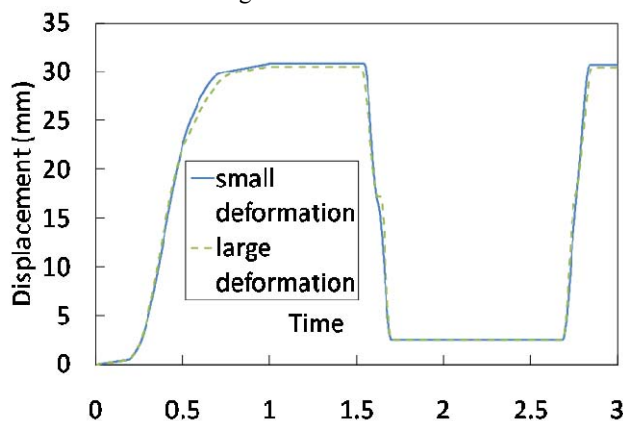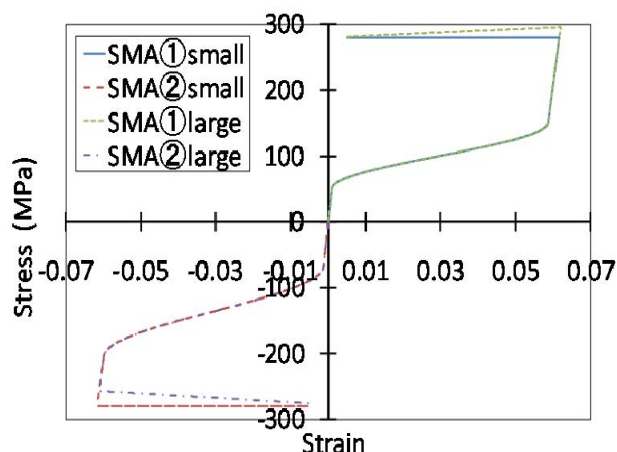Fig.4 Two-bar truss

Fig.5 Time-history of displacement for 2-bar truss

Fig.6 Stress-strain curve for 2-bar truss

Fig. 5 is the time-history of the vertical displacement at the loading point. At t=0~1.0, the displacement due to the martensite transformation of the SMA members is generated with an increase of the load. At t=1.0~2.0, the displacement generated by the martensite transformation disappears, leaving the elastic deformation, due to the inverse (austenite)

transformation with the temperature rising. At t=2.0~3.0, the martensite transformation takes place again, generating the displacement. There is little difference between the results of the small deformation and the large deformation analysis, as the displacement is not so large.

Figure 6 shows the stress-strain curves of the members. In both members, the martensite transformation finishes by the load increase at t=0~1.0. The strains vanish by the inverse (austenite) transformation due to the temperature rise at t=1.0~2.0. The strains are again generated by the martensite transformation due to the temperature drop at t=2.0~3.0. As $\beta = 0.15$ is assumed, the absolute values of the starting and finishing critical stresses for martensite transformation in the member ② (compression) are about 30% higher than those in the member ① (tension).

C. Two-Dimensional Nine-Bar Truss

The two-dimensional nine-bar adaptive truss as shown in Fig. 7 has been analyzed by using the material constants identified in Subsection Ⅲ.A. The members ③ and ⑤ are SMA, while the other members are steel. The cross-sectional area of all the members is 1cm². The load and temperature conditions are given in Fig. 4. The load F(t) increases at t=0~1.0, keeping a constant value at t=1.0~3.0. The temperature keeps a constant value lower than M_f at t=0~1.0, rises over A_f at t=1.0~2.0 and returns back at t=2.0~3.0. The present analysis assumes the symmetric tensile and compressive behavior of SMAs, setting $\beta = 0$ in eq. (7).

Figure 8 is the deformed configuration of the nine-bar truss by the large deformation analysis. At t=1.0, the truss is largely deformed by the martensite transformation due to the loading. At t=1.8, the deformation is almost recovered by the inverse (austenite) transformation due to the temperature rise. At t=2.655, the deformation is again generated by the martensite transformation due to the temperature drop.

Figure 9 is the time-history of the vertical displacement at the loaded point, which is qualitatively similar to the analytical result of Fig. 5 for the two-bar truss. The deformation recovery by the temperature rise after the loading is successfully simulated. Compared with the result calculated by Bandeira et al. [2], there is a little difference in the process of deformation progress and recovery due to the difference of the employed constitutive equations for SMAs. However, the peak values of the displacement agree well with each other. It can be said that the agreement is good as a whole.

Figure 10 is the stress-strain curve for the SMA member ③, which is qualitatively similar to the analytical result in Fig.6 for the two-bar truss member ①. The present analysis program makes the optimum design of adaptive trusses possible for the mechanical property and arrangement of SMA members.
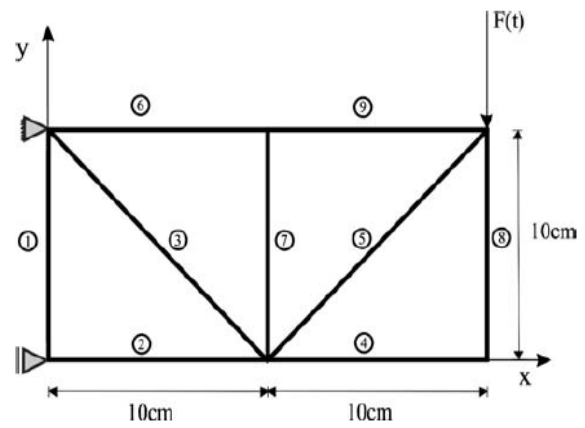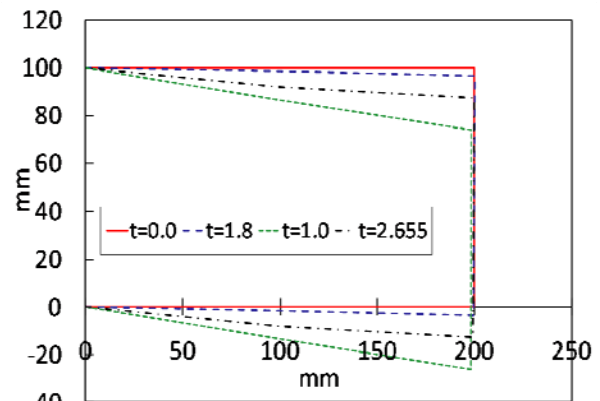

Fig.7 Nine-bar truss
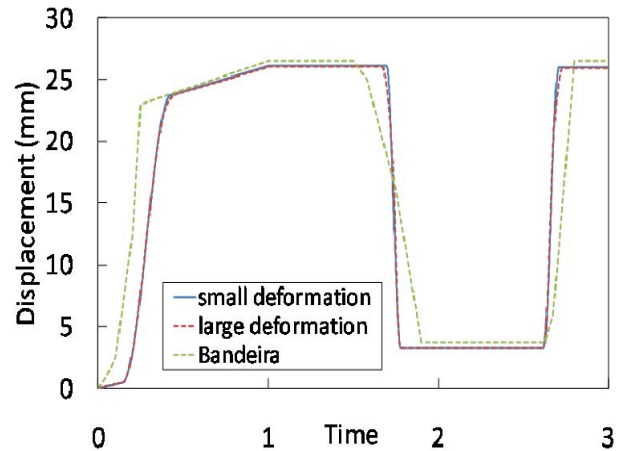

Fig.8 Deformation diagram for 9-bar truss
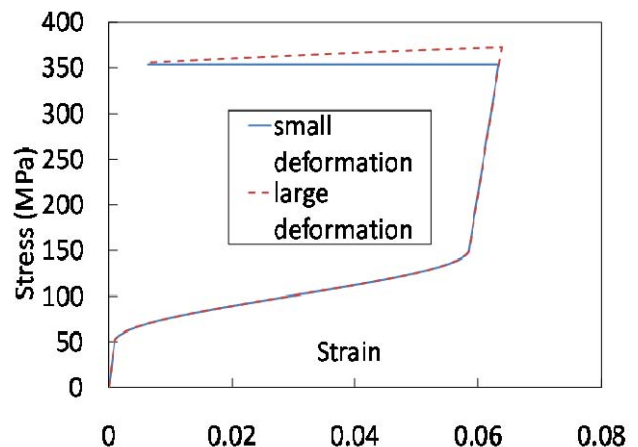

Fig.9 Time-history of displacement for 9-bar truss

Fig.10 Stress-strain curve for 9-bar truss (bar ③)

D. Three-Dimensional Twenty Eight-Bar Truss

The three-dimensional twenty eight-bar adaptive truss as shown in Fig. 11 has been analyzed by using the material constants identified in Subsection Ⅲ.A. The left and right surface structures of the present truss, which are similar to the two-dimensional nine-bar truss in Fig. 7, are connected with the upper and lower surface members. The members ②, ④, ⑩ and ⑫ are SMAs, while the others are steel. The cross-sectional area of all the members is 1cm^2. The loading and temperature conditions are given in Fig. 4. In the present example, the symmetric tensile and compressive behavior is assumed by setting $\beta = 0$ in eq. (7).

Figure 12 shows time-histories of the vertical displacements at the loaded point A and the adjacent point B shown in Fig. 11. The characteristics as an adaptive truss can be understood from the time-history of the displacement (WA) at the loaded point A. The displacement (WB) at the point B is not generated in the small deformation analysis, while a little displacement occurs at the point B in the large deformation analysis, as axial forces are generated in the upper and lower surface members.

Figure 13 is the stress-strain curves for the SMA members ②, ④, ⑩ and ⑫. The stress-strain curves for the member ⑩ and ⑫ are overlapped on those for the members ② and ④.
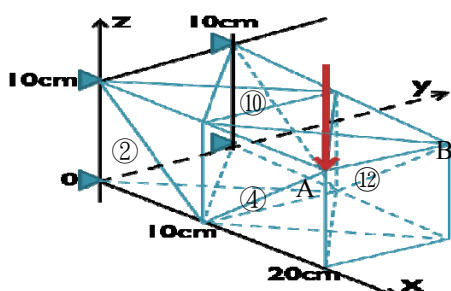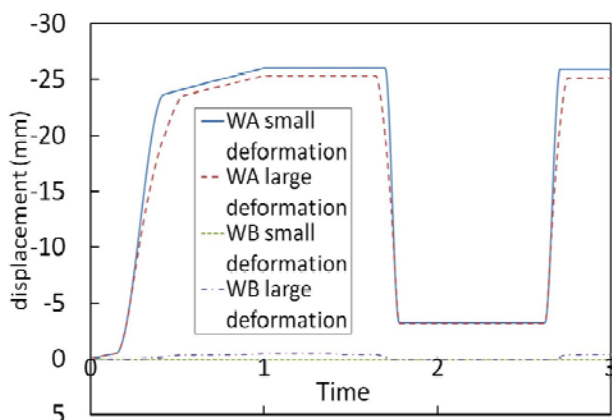

Fig.11 Twenty eight-bar truss

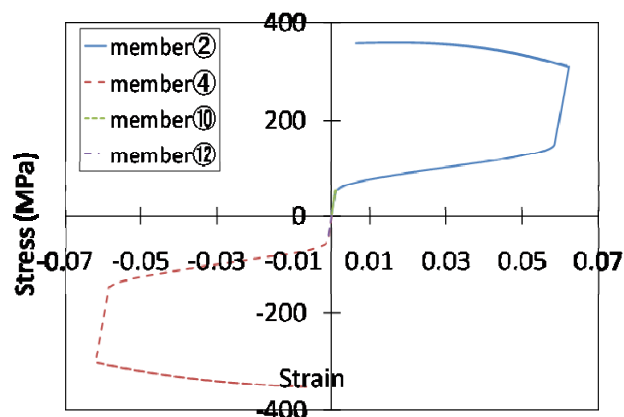Fig.12 Time-history of displacement for 28-bar truss

Fig.13 Stress-strain curve for 28-bar truss

IV. CONCLUSION

In the present study, the incremental finite element analysis procedure has been formulated for the three-dimensional adaptive trusses using SMA members by deriving the tangential form of incremental constitutive equation based on Brinson's constitutive equation extended to consider the asymmetric tensile and compressive behavior.

The formulation has been applied to the superelasticity and shape memory effect behavior analysis of two-dimensional two-bar, nine-bar and three-dimensional twenty eight-bar adaptive trusses using SMA members. The validity and usefulness of the proposed computational algorithm has been demonstrated by the comparison with other numerical solutions and the qualitative consideration.

The present computational procedure, which can simulate the superelasticity and shape memory effect responses of general three-dimensional trusses using SMA members subjected to arbitrary load and temperature histories, is expected to contribute to the rational and efficient design and development of adaptive trusses.

REFERENCES

[1] Hanahara, K. and Tada, Y., Adaptive Truss by Means of Wire Member Actuators, *CD-ROM Proceedings of Dynamics and Design Conference*, JSME No.03-7 (2003).

[2] Bandeira, E. L. et al., Finite Element Analysis of Shape Memory Alloy Adaptive Trusses with Geometrical Nonlinearities, *Arch. Appl.. Mech.*, Vol.76 (2006), pp.133-144.

[3] Paiva, A. et al., A Constitutive Model for Shape Memory Alloys Considering Tensile-Compressive Asymmetry and Plasticity, *Int. J. of Solids and Structures*, Vol.42, No.11-12 (2005), pp.3439-57.

[4] Brinson, L. C., One-Dimensional Constitutive Behavior of Shape Memory Alloys: Thermomechanical Derivation with Non-Constant Material Functions and Redefined Martensite Internal Variable, *J. of Intelligent Material Systems and Structures*, Vol 4, No.2 (1993), pp.229-242.

[5] Toi, Y. et al., Finite Element Analysis of Superelastic, Large Deformation Behavior of Shape Memory Alloy Helical Springs, *Computers and Structures*, Vol.82, No.20-21 (2004), pp.1685-1693.

[6] Toi, Y., *A Course on Computational Solid Mechanics* (*Modeling and Simulation of Materials and Structures*), (2008), pp.56-83, Corona Publishing Company Ltd.

[7] Tobushi, H. et al., Deformation Behavior of Ni-Ti Shape Memory Alloy Subjected to Variable Stress and Temperature, *Continuum Mech Thermodyn*, 3 (1991), pp.79-93.